Role of precipitant species on the coprecipitation for preparing Fe_3O_4 nanoparticles

JIANCHAO MA[a,*], LINGLING WANG[a], YANLI WU[b], XIAODONG ZHAO[d], XIANSHU DONG[a], JILONG ZHANG[a], QINGFANG ZHANG[c], CHEN QIAO[c], QINGLIANG MA[b*]

[a] *College of mining Technology, Taiyuan University of Technology, Taiyuan 030024, Shanxi, PR China*

[b] *Key Laboratory of Coal Science and Technology (Taiyuan University of Technology), Ministry of Education and Shanxi Province, Taiyuan 030024, Shanxi, PR China*

[c] *College of Chemistry and Chemical Engineering, Taiyuan University of Technology, Taiyuan 030024, Shanxi, PR China*

[d] *Nornico Group firmaco, Shanxi North Machine-building CO., LTD, Taiyuan 030024, Shanxi, PR China*

Fe_3O_4 was prepared by adding representative precipitants including NaOH, NH_3•H_2O, N_2H_4•H_2O, Na_2CO_3 and NH_4HCO_3 during the coprecipitation of ferrous and ferric species. The roles of the variable precipitants were explored by X-ray diffraction (XRD), scanning electron microscopy (SEM), vibration sample magnetometer (VSM) and N_2 absorption–desorption analyses. The results indicated that higher pH level favored the formation of a larger volume and stronger saturation magnetizations Fe_3O_4. Thereinto, the strongest saturation magnetization was 89 emu/g. It's also found that Fe_3O_4 nanoparticles were well crystallized using N_2H_4•H_2O because of its oxidation resistance and good precipitability. Furthermore, by the synergistic action of both N_2H_4•H_2O and Na_2CO_3 under mild reaction conditions, the specific surface area of the Fe_3O_4 nanoparticles estimated by the BET equation was up to137.6 m^2/g.

(Received September 02, 2014; accepted November 13, 2014)

Keywords: Magnetite, Coprecipitation, High specific surface area, Strong saturation magnetization

1. Introduction

Nano Magnetite particles (Fe_3O_4) have attracted attention of researchers due to their unique magnetic properties and widespread application in different fields such as magnetic storage devices, catalysis, magnetic refrigeration systems, mineral separation, cancer therapy, magnetic cell separation, and heat transfer applications in drug delivery system [1-5]. Various methods have been reported for the synthesis of Fe3O4 nanoparticles, such as microemulsion [6], hydrolysis [7], hydrothermal/ solvothermal methods [8,9], sol–gel reactions 10, and chemical coprecipitation [11,12]. There into, coprecipitation method is increasingly popular due to its simplicity, inexpensive equipment and potential for large scale production [13]. Nevertheless, it is a great challenge to obtain nanoparticles with satisfied morphology in a controllable manner, as the crystal growth is extremely difficult to control in the complicated reaction system. It's widely acceptable that the role of the precipitant is significantly important as a key contribution to the magnetic particles' morphology, dispersion, size and specific saturation magnetization. However, there has been so far no report of the roles of precipitant species for preparing Fe_3O_4 in the coprecipitation process.

In this work, a series of typical precipitants including NaOH, NH_3•H_2O, N_2H_4•H_2O, Na_2CO_3 and NH_4HCO_3 were added during the coprecipitation of ferrous and ferric species. The effects of doping variable precipitants were studied by X-ray diffraction (XRD), scanning electron microscopy (SEM), vibration sample magnetometer (VSM), and N_2 absorption–desorption analyses.

2. Experimental and methods

All the chemicals were analytical reagents and obtained from Tianjin Kemiou Chemical Reagent Co., Ltd. Commercially available solvents and reagents were used as received without further purification. The Fe_3O_4 nanoparticles were prepared as follows: A 10.0 g precipitant (NaOH, NH_3•H_2O, N_2H_4•H_2O, Na_2CO_3 and NH_4HCO_3) was dissolved in 50 mL H_2O. Therein the concentrations of hydrazine hydrate and ammonium hydroxide was 60 wt. % and 30 wt. %, respectively. An aqueous solution of 3.76 g $FeCl_3$·$6H_2O$ and 1.97 g $FeSO_4$·$7H_2O$ was prepared in 50 mL H_2O. Then, both the solutions were added to a beaker containing 50 mL H_2O and heated at 60 °C for 1 h. Next, the reaction mixture was heated at 100 °C for another 1 h. After cooling to room temperature, the precipitated black solid products were collected using a magnet, washed with water and ethanol several times, and dried in vacuum at 60 °C for 6 h to afford the corresponding Fe_3O_4 nanoparticles.

The Brunauer–Emmett–Teller (BET) specific surface area and pore size measurements were performed by N_2 absorption–desorption at the liquid N_2 temperature using a NOVA2200e automatic surface area and porosity analyzer. The XRD patterns of the samples were recorded using a Rigaku D/max 2500 X-ray diffractometer equipped with Cu Kα radiation (40 kV and 100 mA) in the range 10–90°. The scanning electron microscopy (SEM) images were taken on a LEO1530 scanning electron microscope. The magnetic properties of the products were investigated using a VSM with an applied field between –30,000 and 30,000 Oe at room temperature.

3. Results and discussion

The XRD curves for the as-prepared black powders are illustrated in Fig. 1. For the obtained samples by NaOH, NH_3•H_2O, N_2H_4•H_2O and Na_2CO_3, the diffraction peaks of the samples can be readily assigned to Fe_3O_4, which was in good agreement with the literature [14] and exactly matched with the standard values of Fe_3O_4 (JCPDS NO. 89-4319). Surprisingly, Fe_3O_4 phase can not be clearly observed for the material used NH_4HCO_3 precipitant. Additionally, Calculated from the (3 1 1) diffraction line (35.4°) on the XRD patterns, by use of Scherrer equation, the average diameters of Fe_3O_4 crystals are 55.8±17.3, 34.3±4.6, 33.3±6.4, and 7.1±0.7 nm for the doped precipitant NaOH, NH_3•H_2O, N_2H_4•H_2O and Na_2CO_3, respectively. In order to find the reasons for the phenomena above, the pH values of these precipitant solutions were detected by pH meter. The results show that the pH values are 14, 11, 11, 10 and 8, respectively. Compared with the XRD results, it's found that the pH values dramaticlly affected crystal growth of Fe_3O_4. Experimental results revealed that Fe_3O_4 phase could be easily obtained if the pH value for the reaction solution was more than 8. Interestingly, Fe_3O_4 particles formed better crystallized by the introduction of N_2H_4•H_2O. By observing experiment, the color of reaction liquid by the added N_2H_4•H_2O was black and had no obvious change on the whole process, while the brown solution was transitorily appeared using other precipitants. Considering reaction system, the brown solution might contain Fe^{3+}. Regrettably, the material can not be detected by XRD, it seemed reasonable that Fe^{3+} materials could not be collected by a magnet because of their nonmagnetic properties. Additionally, N_2H_4•H_2O could readily remove the oxygen of solutions by releasing hydrogen and nitrogen at 60 ^oC. Simultaneously, as a strong reducing agent, N_2H_4•H_2O could slow down the speed of oxidation so that the deoxidization behavior of reaction system could take place and avoided the oxygenization of from Fe^{2+} to Fe^{3+}. It implied that N_2H_4•H_2O had the characteristics of both oxidation inhibitor and good precipitant. It was also found that the Fe_3O_4 particle size was increased with the increase of the pH value of the precipitant solution. It implied that a higher pH level resulted in a larger volume of Fe_3O_4.

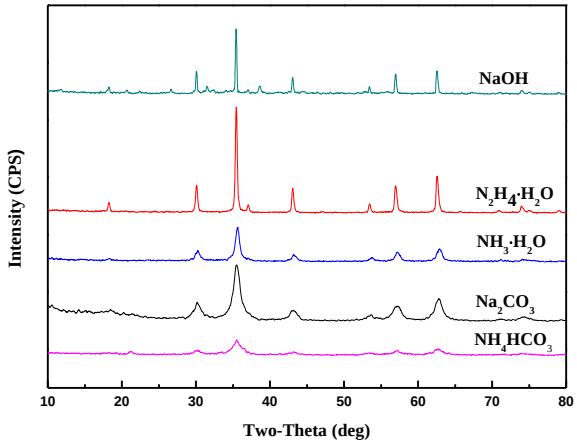

Fig. 1. XRD pattern of Fe_3O_4.

The specific surface areas and pore structural parameters of these Fe_3O_4 materials are summarized in Table 1. Compared with the results in Fig. 1, it was found that the Fe_3O_4 particle size was decreased with the increase of the specific surface areas of the samples, which implied that the lower pH value of a precipitant would favor for the formation of the higher specific-surface-area material. Noteworthily, total pore volume of Fe_3O_4 is significantly larger for decomposable precipitant of heating such as N_2H_4•H_2O, Na_2CO_3 than for indecomposable ones of heating like NaOH and NH_3•H_2O. One possible reason was that decomposable precipitant could come into being large amounts of bubbles, being responsible for the formation of porous structure. Consequently, N_2H_4•H_2O and Na_2CO_3 as the precipitant, were dropwise added together into the reaction system, Fe_3O_4 with a higher surface area (137.6 m^2/g) was obtained, as shown in Table 1. The corresponding N_2 adsorption–desorption isotherm and pore-size distribution curve of the Fe_3O_4 are shown in Fig. 2. The isotherm was classified as type IV with an apparent hysteresis loop in the range 0.3–1.0 P/P°, indicating the presence of mesopores. Furthermore, two main peaks were centered at ~6.5 nm and 12.4 nm. Most of the pores ranged from 3 nm to 30 nm, as shown in the inset of Fig. 2. Posteriorly the pore volume of Fe_3O_4 by the mixture of N_2H_4•H_2O and Na_2CO_3 was nearly equal to the result singly using one of them. In contrast, the average pore diameter became significantly small. These were possible reason why Na_2CO_3 doping N_2H_4•H_2O brought down the pH, promoting the formation of the small pore diameter. Moreover, synergistic action of N_2H_4•H_2O and Na_2CO_3 could cause bimodal pore size. These adequately demonstrated that the type of the precipitant would remarkably influenced pore structural of Fe_3O_4.

Table 1. The BET results for the prepared Fe_3O_4 from various precipitants.

Precipitant	S_{BET}[a](m^2/g)	V_p[b](cm^3/g)	D_p[c](nm)
NaOH	14.9	0.05	14.3
NH_3•H_2O	53.6	0. 09	11.4
N_2H_4•H_2O	72.6	0.27	14.9
Na_2CO_3	104.1	0. 25	9.65
Na_2CO_3+ N_2H_4•H_2O	137.6	0.25	7.21

[a] S_{BET}, The specific surface area.
[b] V_P, Total pore volume.
[c] D_P, Average pore diameter.

Fig. 3 illustrates the SEM micrographs for the produced Fe_3O_4 particles, which have irregular particles shape for all Fe_3O_4 materials. Fig. 3a shows Fe_3O_4 obtained by NaOH, being comprised of some larger block and disintegrating slag particles. While the Fe_3O_4 sizes using Na_2CO_3 are fairly small and more incompact like loose soil, as shown in Fig. 3b. Fig. 3c shows that particles are amorphous or subidiomorphic crystal, and have agglomeration to some extent in appearance by $NaCO_3$ and N_2H_4•H_2O, with the particle diameter of more than 30 nm. As clearly indicated in Fig. 3d by further study, the entire crystal is packed with many fine Fe_3O_4 nanoparticles, indicating that a single nanocrystal had a multicrystal structure. Thus, it's believable that the assembly of small Fe_3O_4 nanoparticles resulted in the formation of its high specific surface area and extensively porous structure, and confirmed BET determinations. The front result can be used to synthesize the Fe_3O_4 with the unique and fine size.

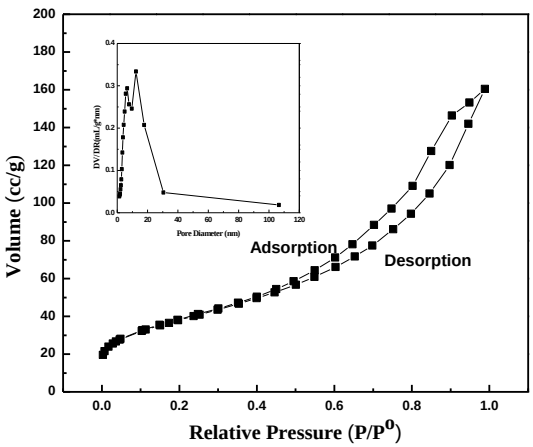

Fig. 2. Nitrogen adsorption–desorption isotherm and the pore size distribution curve (inset) for Fe_3O_4 obtained by the synergistic action of N_2H_4•H_2O and Na_2CO_3.

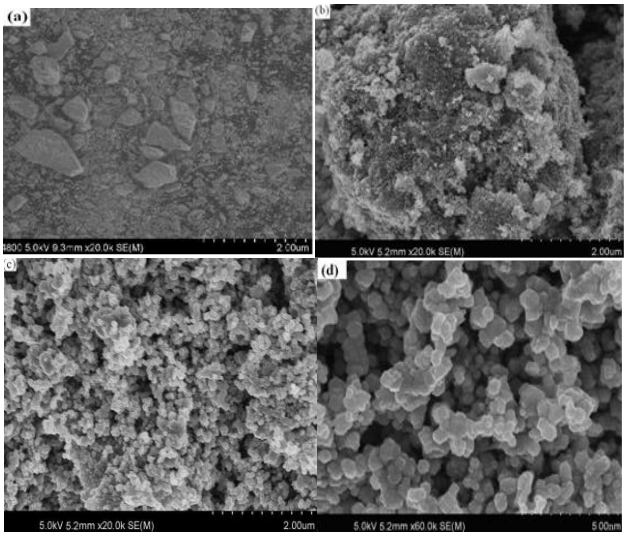

Fig. 3. SEM images of Fe_3O_4 (a) Fe_3O_4 obtained by NaOH, (b) Fe_3O_4 obtained by Na_2CO_3, (c) and (d) obtained by Fe_3O_4 obtained by the synergistic action of N_2H_4•H_2O and Na_2CO_3.

The magnetic properties of the Fe_3O_4 nanoparticles have been measured with the help of the VSM. Fig. 4 shows the corresponding magnetization as a function of magnetic field, or the M versus H curve. Obviously, the magnetic hysteresis loops for all Fe_3O_4 materials are S-like curve, which show no remnant magnetization or coercivity, indicating that the samples exhibited a superparamagnetic behavior at room temperature. Generally, magnetite particles with sizes below 30 nm can have superparamagnetic properties [15]. The average sizes of Fe_3O_4 materials were more than 30 nm, but they still exhibited superparamagnetic behavior. Nevertheless, apart from the particle size and crystallinity, there were many factors such as surface spin-canting, surface disorder, surface ligands, cation site distribution, and stoichiometry deviation that affected the magnetic properties of nanoparticles, even when synthesized by the same approach [16]. Thus it could be understood that the Fe_3O_4 nanoparticles obtained by different precipitant possessed superparamagnetic properties. Additionally, the saturation magnetizations (Ms) of the magnetite nanocrystalline using NaOH, N_2H_4•H_2O, Na_2CO_3 and the mixture of N_2H_4•H_2O and Na_2CO_3 is about 89, 52, 30, 54 emu/g, respectively. Compared with the SEM and XRD results, it could be found that the magnetic force acting on a particle is in a certain proportional to the particle volume. In the other hand, a larger volumetric Fe_3O_4 generally possessed a better magnetic response. If the particles were too small, their magnetic tractive forces in a field gradient will not be large enough to overcome Brownian motion, and no separation will occur. For Fe_3O_4 extrapolations from the behavior of the bulk material suggested that the critical size for separation was more than 30 nm for the case of an isolated (nonaggregated) particle.

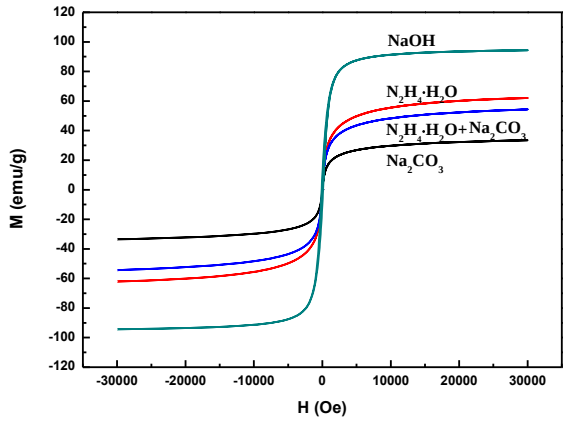

Fig. 4. Hysteresis curve of Fe_3O_4.

4. Conclusions

Representative precipitants including NaOH, NH_3•H_2O, N_2H_4•H_2O, Na_2CO_3 and NH_4HCO_3 were used in the coprecipitation of Fe^{3+} and Fe^{2+} agents, the roles of doping precipitants were systematically studied. Experimental result indicated that higher pH levels resulted in a larger volume of Fe_3O_4 particles, which could be responsible for the size and the saturation magnetization of Fe_3O_4. It's also convinced that the precipitation types would affected morphological features of Fe_3O_4. The Fe_3O_4 nanoparticles were well crystallized using N_2H_4•H_2O on account of its characteristics of oxidation inhibitor and good precipitant. Furthermore, the specific surface area of the Fe_3O_4 nanoparticles estimated by the BET equation was 137.6 m^2/g, with the introduction of N_2H_4•H_2O and Na_2CO_3. It could be also found that a larger volumtric Fe_3O_4 generally possessed a stronger magnetic response. These features are beneficial for their application in some special field such as adsorbents, recoverable catalysts, drug targets, and so on.

Acknowledgments

This work was supported by the National Natural Science Foundation of China (No. 51204119) and the Natural Science Foundation of Shanxi Province (No. 2014021015-4).

References

[1] P. Panneerselvam, N. Morad, K.A. Tan, J. Hazard. Mater. **186**, 160 (2011).
[2] R.-Y. Hong, J.-H. Li, S.-Z. Zhang, H.-Z. Li, Y. Zheng, J.-m. Ding, D.-G. Wei, Appl. Surf. Sci. **255**, 3485 (2009).
[3] M. Gao, W. J. Condens. Matt. Phys. **1**, 49 (2011).
[4] L. Wang, J. Li, Q. Jiang, L. Zhao, Dalton. Trans. **41**, 4544 (2012).
[5] A. Wu, P. Ou and L. Zeng, Nano **5**, 245 (2010).
[6] QI.Huang, D. Zhang, H. zhang, S. wang, Z.Sun, J. Wang and F.Liu, J. Optoelectron. Adv. Mat. **6**(7), 456 (2012), L. Han and Y. Wei, Mater. Lett. **70**, 1 (2012).
[8] R. Fana, X.H. Chen, Z. Gui, L.Liu, Z.Y. Chen, Mater. Res. Bull. **36**, 497 (2001).
[9] Z. Cheng, X. Chu, H. Zhong, J. Yin, Y. Zhang and J. Xu, Mater. Lett. **76**, 90 (2012).
[10] L.H. Shen, J.F. Bao, D. Wang, Y.X. Wang, Z.W. Chen, L. Ren, X. Zhou, X. B. Ke, M. Chen, A.Q. Yang, Nanoscale 5, 2133 (2013).
[11] R.G. RuizMoreno, A.I. Martínez, C. Falcony, R. Castro-Rodriguez, P. Bartolo-Pérez, M. Castro-Román, Mater. Lett. **92**, 181 (2013).
[12] Y. Wei, B. Han, X. Hu, Y. Lin, X. Wang, X. Deng, Procedia Eng. **27**, 632 (2012).
[13] H. Meng, Z. Zhang, F. Zhao, T. Qiu, J. Yang, Appl. Surf. Sci. **280**, 679 (2013).
[14] F. Chen, S. Xie, J. Zhang, R. Liu, Mater. Lett.**112**, 177 (2013).
[15] Y. Hwang, S. Angappane, J. Park, K. An, T. Hyeon, J.-G. Park, Curr. Appl. Phys. **12**, 808 (2012).
[16] J. Salado, M. Insausti, I. Gil de Muro, L. Lezama, T. Rojo, J. Non-Cryst. Solids **354**, 5207 (2008).

*Corresponding author: majianchao@tyut.edu.cn
maqingliang@tyut.edu.cn